

**MODIFIED HOPFIELD NEURAL NETWORK
CLASSIFICATION ALGORITHM FOR
SATELLITE IMAGES**

By

AHMED ASAL KZAR

**Thesis submitted in fulfilment of the requirements
for the degree of
Doctor of Philosophy**

May 2016

ACKNOWLEDGEMENT

I thank firstly Allah, which supported me the power and the capabilities that assist me in my study, and who helped me in solving the several problems that faced me during the study period, and who guided me to the success.

Then I thank my supervisor Prof. Mohd Zubir bin Mat Jafri who gave my all successful guidelines and advice that aided me during the study time until the end. Also, he endured all my problems that faced me during this time. So, I wish to thank and appreciate my co-supervisors: Assoc. Prof. Lim Hwee San, Prof. Ali Abid D. Al-Zuky, and Dr. Kussay Nugamesh Mutter, about the guidelines, help, and encouragement for me to complete this achievement.

I offer my regards and blessings to all of persons: lecturers, students, brothers, and friends for their assistant such as Dr. Emad, Dr. Hazim, Dr. Faiz, Dr. Ghayth, Dr. Mehaj, Dr. Saumi, Haider, Rasim and, Anwar. I would also like to express my gratitude to my wife Zainab Basim for her patience and help. I express my big appreciation to university of Kufa, which offered me this opportunity. I thank Malaysia, which received me and my family, so, for staying and study. Special thanks for USM for giving me the study opportunity. I pray to Allah to bless and support each person in our world.

Ahmed

TABLE OF CONTENTS

	Page
ACKNOWLEDGEMENT	ii
TABLE OF CONTENTS	iii
LIST OF TABLES	viii
LIST OF FIGURES	xi
LIST OF SYMBOLS AND ABBREVIATIONS.....	xv
ABSTRAK.....	xvii
ABSTRACT	xviii
CHAPTER ONE - INTRODUCTION.....	1
1.1 Overview	1
1.2 Water quality	2
1.2.1 Water Quality Mapping	3
1.2.2 Water Quality Parameters	3
1.2.2.(a) Total Suspended Solids (TSS).....	4
1.2.2.(b) Chlorophyll.....	4
1.2.3 Water Quality Assessment	5
1.3 Remote Sensing Techniques	5
1.4 Artificial Neural Network	8
1.5 Image Classification.....	9
1.5.1 Supervised Classification.....	9
1.5.2 Unsupervised Classification.....	10
1.6 Mapping	11
1.7 The Physical Concept of the Used Image	12

1.7.1	The Physical Concept of the Binary Image	12
1.7.2	The Physical Concept of the Colour Image	12
1.8	Problem Statement	13
1.9	Research Objectives	14
1.10	Scope of the Study	15
1.11	Thesis Organization	15
CHAPTER TWO - LITERATURE REVIEW AND THE HOPFIELD NEURAL NETWORK.....		17
2.1	Literature Review	17
2.1.1	Hopfield Neural Network Components	17
2.1.1.(a)	Vector Size and HNN Capacity.....	18
2.1.1.(b)	Self-Connection Architecture in HNN.....	20
2.1.1.(c)	Hopfield as Feedforward Network.....	21
2.1.1.(d)	Energy Function	21
2.1.2	HNN for Multicolour Images.....	23
2.1.3	ANN for Water Quality.....	25
2.1.4	HNN with Remote Sensing for Water Quality	27
2.1.5	Satellite Images for Water Quality Mapping	28
2.2	Hopfield Neural Network (HNN)	29
2.2.1	Algorithm of Hopfield Neural Network (HNN)	29
2.2.2	Hopfield Neural Network Applications	30
2.2.3	Hopfield Neural Network Limitations	32
2.2.4	HNN Algorithm for Colour Images	33
2.2.5	Disadvantages and Limitations of MHNN.....	35
2.3	Summary	36

CHAPTER THREE - DEVELOPING OF MHNN FOR SATELLITE IMAGES CLASSIFICATION..... 37

3.1 Introduction 37

3.2 The MHNNA Architecture 38

3.3 MHNNA for Satellite Images 39

 3.3.1 Learning Phase 39

 3.3.1.(a) The Vector of MHNNA 39

 3.3.1.(b) Initialization of the Learning Weights of MHNNA 43

 3.3.2 Convergence Phase 45

 3.3.2.(a) Energy Function (*E*) of MHNNA 47

 3.3.3 General Formula for the Majority Description (MD) 59

3.4 Summary 61

CHAPTER FOUR - METHODOLOGY OF MHNNA CLASSIFICATION FOR WATER QUALITY MAPPING 62

4.1 Introduction 62

4.2 The Required Components 64

 4.2.1 Hardware Components 64

 4.2.2 Software Components 64

4.3 Study Areas 64

 4.3.1 Penang Strait 65

 4.3.2 Coastal Waters of Langkawi Island 66

4.4 Validation 67

4.5 The Adopted Remote Sensing Images 68

 4.5.1 Thailand Earth Observation System (THEOS) Images 68

 4.5.1.(a) THEOS 12-11-2009 Image 70

 4.5.1.(b) THEOS 29-1-2010 Image 72

4.5.2	Advanced Land Observation Satellite (ALOS) Images	74
4.5.2.(a)	ALOS 18-1-2010 Image.....	76
4.5.2.(b)	ALOS Mosaic Image.....	78
4.6	Giving Bands Ratios	81
4.7	Masking.....	81
4.8	Sample Size.....	82
4.9	MHNNA with Satellite Images for Water Quality Mapping.....	83
4.9.1	MHNNA as Classifier for Water Pollutants Concentrations ..	83
4.9.1.(a)	Algorithm 1	83
4.9.1.(b)	Algorithm 2	86
4.9.1.(c)	Testing of MHNNA with the Noise	89
4.9.2	MHNNA for Estimation of Water Pollutants Concentrations	90
4.9.2.(a)	The Developing Assumption.....	91
4.9.2.(b)	Algorithm 3	97
CHAPTER FIVE - RESULTS AND DISCUSSIONS		101
5.1	Introduction.....	101
5.2	Results of the MHNNA.....	102
5.2.1	Testing of MHNNA for Colour Image	102
5.2.1.(a)	Testing of MHNNA for Classification of Colour Image .	102
5.2.1.(b)	Testing of MHNNA for Classification of Colour Water Image	104
5.2.2	The Physical Meaning of the Pollutants Results.....	106
5.2.3	The Contributions of MHNNA for Classification	106
5.2.4	Validation.....	113
5.2.5	Test MHNNA with Noise	113
5.2.5.(a)	Testing Noise with THEOS Image.....	114

5.2.5.(b) Testing Noise with ALOS Image	118
5.2.6 Results of the Classification of Pollutants by MHNNA	121
5.2.6.(a) Results of Algorithm 1	121
5.2.6.(b) Results of Algorithm 2	155
5.2.7 Results of the Estimation of the Pollutant Concentration	161
5.2.7.(a) Applying MHNNA for the Estimation of TSS.....	161
5.2.7.(b) Applying MHNNA for the Estimation of Chlorophyll	164
5.3 Summary	166
CHAPTER SIX - CONCLUSIONS AND RECOMMENDATIONS FOR FUTURE WORK	167
6.1 MHNNA as a Classifier for Satellite Images.....	167
6.2 Validation Data	168
6.3 MHNNA Efficiency	169
6.3.1 Testing MHNNA with Noisy Images	169
6.3.2 Testing MHNNA with Several Satellite Images.....	169
6.4 MHNNA for the Estimation of Pollutants Concentrations	169
6.5 Recommendations for Future Work.....	170
REFERENCES.....	171
APPENDICES	188
LIST OF PUBLICATIONS.....	191

LIST OF TABLES

	Page
Table 3.1: All the possible vectors with their weight matrices [91].	43
Table 3.2: All possible energy function values of the MHNNA.	50
Table 4.1: Technical specifications of THEOS.	69
Table 4.2: THEOS Characteristics.	70
Table 4.3: The Samples Values of the validation data for the THEOS 12-11-2009 image: TSS and chlorophyll concentrations values and their locations.	72
Table 4.4: The Samples Values of the validation data for the THEOS 29-1-2010 image: TSS concentrations values and their locations.	74
Table 4.5: Technical specifications of ALOS.	75
Table 4.6: ALOS Characteristics.	76
Table 4.7: The Samples (TSS) Values of the validation data for ALOS 18-1-2010 image.	77
Table 4.8: The Sample Values of the validation data for the ALOS mosaic image.	80
Table 5.1: Classification samples and test samples for TSS mapping through a comparison between MHNNA as feedback and MHNNA as feedforward.	108
Table 5.2: Comparison between the accuracy of MHNNA as Feedback and the accuracy of MHNNA as Feed forward.	108
Table 5.3: Proving the advantage of using Wb in MHNNA.	111
Table 5.4: Comparison between the accuracy of MHNNA with/without Wb .	111
Table 5.5: Comparison between the accuracy of MHNNA as a Non-Zero-diagonal architecture and the accuracy of MHNNA as a Zero-diagonal architecture.	112
Table 5.6: Comparison between the accuracy of MHNNA and the accuracy of the Min-dis classifier for TSS mapping with SPN noise for the THEOS image through the mean of R and the mean of RMSE.	116
Table 5.7: Comparison between the accuracy of MHNNA and the accuracy of the Min-dis classifier for Chlorophyll mapping with the SPN noise	

	for the THEOS image and measuring the result through the mean R and the mean RMSE.	118
Table 5.8:	Comparison between the accuracy of MHNNA and the accuracy of the Min-dis classifier for TSS mapping with SPN noise for the ALOS 18-1-2010 image, through the mean of R and the mean of RMSE.	120
Table 5.9:	Comparison between MHNNA and the Min-dis classifier for the TSS mapping of the image through classification samples and THEOS 12-11-2009 test samples.	124
Table 5.10:	Comparison between MHNNA and the Min-dis classifier for the TSS mapping by THEOS 12-11-2009 through using R and RMSE.	124
Table 5.11:	Comparison between MHNNA and the Min-dis classifier for the chlorophyll mapping with the THEOS 12-11-2009 image through the classification of the samples and test samples.	127
Table 5.12:	Comparison between MHNNA and the Min-dis classifier for chlorophyll mapping by THEOS 12-11-2009 through R and RMSE.	127
Table 5.13:	The adopted ratios for the bands used for the TSS mapping of THEOS 29-1-2010.	135
Table 5.14:	Comparison between MHNNA and the Min-dis classifier for the TSS mapping by the THEOS 29-1-2010 image through Classification samples and test samples.	138
Table 5.15:	Comparison between MHNNA and the Min-dis classifier for the TSS mapping by the THEOS 29-1-2010 image through R and RMSE.	139
Table 5.16:	The adopted ratios for the bands used for the TSS mapping of the ALOS 18-1-2010 image.	139
Table 5.17:	Comparison between MHNNA and the Min-dis classifier for TSS mapping of the ALOS 18-1-2010 image through Classification samples and test samples.	142
Table 5.18:	Comparison between MHNNA and the Min-dis classifier for the TSS mapping of the ALOS 18-1-2010 image through R and RMSE.	143
Table 5.19:	The adopted ratios for the bands used for the TSS mapping of the ALOS mosaic image.	149
Table 5.20:	Comparison between MHNNA and the Min-dis classifier for TSS mapping using the ALOS mosaic image through Classification samples and test samples.	153

Table 5.21: Comparison between MHNNA and the Min-dis classifier for TSS mapping using the ALOS mosaic image and measuring the performance with R and RMSE.	154
Table 5.22: Comparison between MHNNA with the second representation vector and Min-dis classifier for the TSS mapping by the THEOS 12-11-2009 image through Classification samples and test samples.	157
Table 5.23: Comparison between MHNNA with the second representation vector and the Min-dis classifier for TSS mapping by the THEOS 12-11-2009 image through R and RMSE.	157
Table 5.24: Comparison between MHNNA with the second representation of the network vector and the Min-dis classifier for chlorophyll mapping by the THEOS 12-11-2009 image via the Classification samples and test samples.	160
Table 5.25: Comparison between MHNNA with the second representation of the network vector and the Min-dis classifier for chlorophyll mapping by the THEOS 12-11-2009 image via R and RMSE.	160
Table 5.26: Comparison between MHNNA as an estimator of the pollutant concentrations and Multi-regression for the TSS mapping by the THEOS 12-11-2009 image through R and RMSE.	163
Table 5.27: Comparison between MHNNA as an estimator of the pollutant concentrations and multi-regression for chlorophyll mapping by the THEOS 12-11-2009 image through R and RMSE.	165

LIST OF FIGURES

	Page
Figure 1.1: Electromagnetic Spectrum.	6
Figure 2.1: An example of the Hopfield network behaviour when it is used as content-addressable memory [92].	31
Figure 2.2: Local and global minima [144].	32
Figure 2.3: Bitplanes that represent the bands of RGB image.	34
Figure 3.1: The architecture of the MHNNA.	39
Figure 3.2: All possible vectors and the orthogonality phenomenon.	41
Figure 3.3: A band range in decimal and binary systems with a demonstration of the weight of bits.	52
Figure 3.4: An example shows two samples (patterns) that are known and one unknown pattern with their conversion from decimal to binary and then to the bipolar system and the sequence of W_b that are considered in MHNNA.	53
Figure 4.1: Research methodology flow.	63
Figure 4.2: The first study area (Penang strait).	65
Figure 4.3: The second study area (Langkawi Island) [167].	66
Figure 4.4: Thailand Earth Observation System (THEOS).	69
Figure 4.5: The raw satellite image (THEOS 12-11-2009) and sampling locations.	71
Figure 4.6: The raw satellite image (THEOS 29-1-2010) and sampling locations.	73
Figure 4.7: A view of ALOS.	75
Figure 4.8: The raw satellite image (ALOS 18-1-2010) and sampling locations.	77
Figure 4.9: Raw ALOS images acquired on the dates: (a) 18-1-2010 (b) 16-2-2010 to produce a mosaicked image.	78
Figure 4.10: The new ALOS mosaicking with its sample locations.	79
Figure 4.11: The relationship of the energy function values to the concentration values.	92

Figure 4.12: Linear relationship between the red band and the TSS concentrations.	93
Figure 4.13: Linear relationship between the green band and the TSS concentrations.	93
Figure 4.14: Linear relationship between the blue band and the TSS concentrations.	94
Figure 5.1: Test MHNNA on the colour image and perform a comparison with Min-dis.	103
Figure 5.2 : Testing MHNNA for colour water images and comparison with Min-dis.	105
Figure 5.3: Proving the advantage of MHNNA as a feedforward network for classification: (A) Original image. (B) MHNNA as a feedback net. (C) MHNNA as a feedforward net.	107
Figure 5.4: Proving the advantage of Wb in MHNNA: (A) Original image. (B) MHNNA without Wb . (C) MHNNA with Wb .	110
Figure 5.5: Test MHNNA with salt-and-pepper noise and in comparison with Min-dis, applying it to the THEOS image for the TSS pollutant and measuring the accuracy by the correlation coefficient (R).	114
Figure 5.6: Test MHNNA with salt-and-pepper noise and perform a comparison with Min-dis, applying it to the THEOS image for TSS pollution and measuring the accuracy by root Mean square error (RMSE).	115
Figure 5.7: Testing MHNNA with salt-and-pepper noise and comparing it with Min-dis, applied to the THEOS image for the Chlorophyll pollutant, with the accuracy measured by the correlation coefficient (R).	117
Figure 5.8: Test MHNNA with salt-and-pepper noise and perform a comparison with Min-dis, applying it to the THEOS image for the Chlorophyll pollutant and measuring the accuracy with the Root Mean Square Error (RMSE).	117
Figure 5.9: Testing MHNNA with salt-and-pepper noise and performing a comparison with Min-dis, applied to the ALOS 18-1-2010 image for the TSS pollutant and measuring the accuracy with the correlation coefficient R.	118
Figure 5.10: Testing of MHNNA with salt-and-pepper noise and performing a comparison with Min-dis, applying it to the ALOS 18-1-2010 image for the TSS pollutant and measuring the accuracy with the RMSE.	119
Figure 5.11: Choosing the sample size for MHNNA with the THEOS 12-11-2009 image for the TSS map.	122
Figure 5.12: TSS map. (A) THEOS 12-11-2009 image. (B) Min-dis classifier result. (C) MHNNA result.	123

Figure 5.13: Choosing the sample size for MHNNA with the THEOS 12-11-2009 image for the chlorophyll map.	125
Figure 5.14: Chlorophyll map. (A) THEOS 12-11-2009 image. (B) Min-dis classifier result. (C) MHNNA result.	126
Figure 5.15: Proving the ability of MHNNA for classification through the closeness between the mean and the standard deviation of the samples (classes) and the raw image data that followed produced classes by the application of MHNNA to THEOS 12-11-2009 image.	129
Figure 5.16: Proving the ability of MHNNA to perform classification by the error value between the mean of each band of (red, green, and blue) in each sample and the mean of these bands in each class.	131
Figure 5.17: Analysis of the raw data of each band that followed the produced classes by MHNNA through the probability for each value of these data.	132
Figure 5.18: Analysis of the energy function values of each band of each class of whole water data in the adopted image through using MHNNA.	133
Figure 5.19: The areas of the classes (by square kilometre) of the TSS pollutant concentrations in Penang strait, Malaysia, on the date of 12-11-2009, from applying MHNNA on the THEOS image.	134
Figure 5.20: Choosing the sample size for MHNNA with the THEOS 29-1-2010 image for the TSS map.	136
Figure 5.21: TSS map: (A) Original THEOS 29-1-2010 image. (B) Result of Min-dis classifier. (C) Result of MHNNA.	137
Figure 5.22: Choosing the sample size for MHNNA with the ALOS 18-1-2010 image for the TSS mapping.	140
Figure 5.23: TSS map: (A) Original ALOS 18-1-2010 image. (B) Result of the Min-dis classifier. (C) Result of MHNNA.	141
Figure 5.24: Proving the ability of MHNNA for classification through the closeness between the mean and the standard deviation of the samples and the raw image data that followed produced classes by MHNNA being applied to ALOS 18-1-2010	144
Figure 5.25: Proving the ability of MHNNA to perform classification by the error value between the mean of each band of (blue, green, and red) in each sample and the mean of these bands in each class.	145
Figure 5.26: Analysis of the raw data of each band, which followed the produced classes by MHNNA through the probability of each value of these data.	146

Figure 5.27: Analysis of the energy function values of each band of each class for all of the water pixels in the adopted image through using MHNNA.	147
Figure 5.28: The areas of the classes (by squared kilometre) of the TSS pollutant concentrations in Langkawi Island, Malaysia, on the date of 18-1-2010, by applying MHNNA on the ALOS image.	148
Figure 5.29: Choosing the sample size for MHNNA with the ALOS mosaic image for the TSS map.	150
Figure 5.30: TSS map: (A) Original ALOS mosaic image. (B) Result of the Min-dis classifier. (C) Result of MHNNA.	151
Figure 5.31: Choosing the sample size for MHNNA with the second representation vector and applying it to the THEOS 12-11-2009 image for a TSS map.	155
Figure 5.32: TSS map: (A) Original THEOS 12-11-2009 image. (B) Result of Min-dis classifier. (C) Result of MHNNA.	156
Figure 5.33: Choosing the sample size for MHNNA with the new vector and applying it to the THEOS 12-11-2009 image for the chlorophyll map.	158
Figure 5.34: Chlorophyll map. (A) Original THEOS 12-11-2009 image. (B) Result of Min-dis classifier. (C) Result of MHNNA.	159
Figure 5.35: TSS map by applying developed MHNNA to estimate the pollutant concentrations, on the THEOS 12-11-2009 image.	162
Figure 5.36: The achievement of the developed MHNNA for estimating the TSS concentration compared with the validation data, as applied to the THEOS 12-11-2009 image.	163
Figure 5.37: Chlorophyll map by applying the developed MHNNA for the estimation of the pollutant concentrations, on the THEOS 12-11-2009 image.	164
Figure 5.38: The achievement of the developed MHNNA for the estimation of the chlorophyll concentration compared with the validation data, as applied to THEOS 12-11-2009.	165

LIST OF SYMBOLS AND ABBREVIATIONS

ALOS	Advanced Land Observation Satellite
ANN	Artificial Neural Network
AOI	Area of Interest
BAM	Bidirectional associative memories
BOD	Biological Oxygen Demand
C_I	Concentration of the Image pixel
C_S	Concentration of the Sample
E	Energy function
E^b	Summation of Energy Function values of the blue band
E^g	Summation of Energy Function values of the green band
E^r	Summation of Energy Function values of the red band
FLC	Fuzzy Logic Controller
GPS	Global Positioning System
HNN	Hopfield Neural Network
HTNN	Hopfield Type Neural Network
ICH	Information Capacity of Hopfield neural network
LMI	Linear Matrix Inequality
$mdkv$	majority description of known vector
$mduv$	majority description of unknown vector

m_I	Mean of intensities values of Image pixels
m_s	Mean of intensities values of sample pixels
MHNN	Modified Hopfield Neural Network
MHNNA	Modified Hopfield Neural Network Algorithm
MLP	Multi-Layer Perceptron
N_{binary}	Number in binary system
N_{bipolar}	Number in bipolar system
PV	Photovoltaic
RMSE	Root Mean Square Error
ROSIS	Reflective Optics System Imaging Spectrometer
SEF	Summation of Energy Function values of the bands: red, green, blue
SEF_I	Summation of energy function values of the Image
SEF_s	Stander summation of energy function values of the sample
THEOS	Thailand Earth Observation System
TSS	Total Suspended Solids
V	Vector of the Hopfield neural network
Wb	Weight of bits
W_{ij}	Learning Weight

ALGORITMA PENGKELASAN JARINGAN NEURAL HOPFIELD TERUBAHSUAI UNTUK IMEJ SATELIT

ABSTRAK

Air adalah bahan yang penting bagi kehidupan makhluk di atas muka bumi ini. Aktiviti manusia dan pengaruh alam semula jadi memberi kesan terhadap kualiti air, dan ia dianggap satu daripada masalah terbesar yang membelenggui kehidupan. Beberapa teknik telah digunakan bagi menangani masalah ini, kecekapan kaedah penderiaan jauh terbukti dalam pemetaan kualiti air. Sementara itu, rangkaian neuro buatan turut terbukti kecekapannya sebagai model matematik dengan teknik penderiaan jauh bagi pemetaan kualiti air. Rangkaian neuro Hopfield adalah jenis rangkaian yang paling ringkas, mudah, cepat dan berkesan. Namun demikian, rangkaian ini tidak dapat digunakan dengan imej berwarna. Justeru, penyelidik cuba menangani masalah ini melalui pengubahsuaian pada jenis rangkaian tersebut, dan dikenali sebagai MHNNA, yang sesuai bagi pengelasan imej berwarna. Pengubahsuaian yang dilakukan adalah berdasarkan tiga faktor: matriks berat diagonal sifar, HNN sebagai rangkaian *feedforward*, dan berat bit dalam persamaan fungsi tenaga. Ia dapat menangani masalah minimum setempat, penggunaan masa, dan juga dengan sejumlah jalur imej. Kecekapan algoritma baru dengan sampel imej satelit warna bagi pemetaan kualiti air terbukti berdasarkan kesahihan data. MHNNA telah diuji dengan imej hinggar (noisy images) dan terbukti kelancarannya sehingga (66%) daripada (30) kuantiti hinggar yang ditambah. Dua imej daripada setiap jenis THEOS dan ALOS dengan tarikh yang berbeza diambil kira bagi imej penderiaan jauh. Di samping itu, satu algoritma baru dibangunkan untuk menganggar kepekatan bahan pencemar melalui tambahan langkah baru pada MHNNA. Kecekapan algoritma dengan imej satelit warna bagi pemetaan kualiti air terbukti berdasarkan kesahihan data, yang menunjukkan nilai pekali korelasi (R) yang amat tinggi dan mencecah 0.996 untuk TSS, dan nilai terendah punca min kuasa dua ralat (root mean square error, RMSE), mengurang sehingga 0.564 mg/m³ untuk klorofil, apabila dibandingkan dengan kaedah standard, yang merupakan pengelas jarak minimum bagi anggaran pengelasan dan multiregresi.

MODIFIED HOPFIELD NEURAL NETWORK CLASSIFICATION ALGORITHM FOR SATELLITE IMAGES

ABSTRACT

Water is an essential material for living creatures. Human activities and natural influences have an effecting on water quality, and this is considered one of the largest problems facing living forms. Several techniques have been used to address this problem. Remote sensing images have proven their efficiency for water quality mapping. Artificial neural networks have been proven their efficiency as mathematical models with remote sensing techniques for water quality mapping. Hopfield neural network type is a simple, common, fast and efficient network, but, this network is unable to deal with colour images. The researcher in this work addressed this problem through a new modification of this network type. Named MHNNA, which is suitable for classification of colour images. The modification is based on three factors: a zero diagonal weight matrix, HNN as a feedforward network, and weights of bits in the energy function equation. It solves the local minimum problem, time consuming, and it deals with the numbers of image bands deeply. The efficiency of the new algorithm with the sampled color satellite images for water quality mapping has been proven by data validation. MHNNA has been tested with noisy images, proving steadfast until 66% of 30 quantities of noise were added. Two images of THEOS type and two of ALOS type with different dates have been considered for remote sensing images. In addition, a new algorithm is developed to estimate pollutant concentrations by adding new steps to MHNNA for estimation. The efficiency of the algorithm with the colour satellite images for water quality mapping has been proven via validation data that showed higher values of the correlation coefficient (R), reaching up to 0.996 for TSS and lower values of the root mean square error (RMSE), decreasing to 0.564 mg/m³ for chlorophyll, when compared with the standard method, which is the minimum distance classifier for classification and multi-regression for estimation.

CHAPTER ONE

INTRODUCTION

1.1 Overview

Water is the most precious natural resource on Earth, covering approximately three quarters of it. Pure water has no colour, taste, or smell. It forms the world's oceans, seas, lakes, streams, rain, and ground water. It is the major constituent of the fluids and the lifeblood of living creatures. Sustained economic development in any country in the world depends greatly on water. Water resources and environmental management are essential for sustaining the quality of life on Earth. Therefore, the deterioration of water quality represents a large environmental problem for living creatures. Water quality on the surface or in the ground has been affected by human activities or natural influences or both [1]. The most important natural influences are geological, hydrological and climatic [2]. Human activities have the potential to impair water quality, thus reducing the utility of water as a resource, and degrade aquatic ecosystems [3]. Studies in several locations have investigated the effects of water quality [4, 5]. To date, the deterioration of water quality is still occurring in many water bodies of the world. The first step of solving this problem requires monitoring and assessment studies for water pollutants, analysis of water pollutants, and identification of the sources or causes of the pollutants to initiate suitable solutions to stop, reduce or avoid them. Scientists and researchers have continuously contributed to these requirements, so several techniques have been introduced to address water quality [6-9], as the problem of water quality has garnered interest from scientists and researchers, especially when water has dynamic properties as a liquid, compared with the other parts of the Earth's

surface that have static properties for long periods of time. For this, the mapping of water quality as a water quality technique has particular applicability.

Previous studies have proved that the best techniques for water quality are remote sensing techniques [10]. The traditional sampling method, which uses a ship, boat, or marine vehicle for water quality, requires high time consumption, high cost [11-13], and high exertion of effort; also, the consumed time may give inexact readings because of dynamic changes in the water pollutant concentrations during the long period of time required to examine the entire study area. Remote sensing techniques have overcome all these requirements [14, 15]. The use of remote sensing data for water quality yields better results [16]. With remote sensing data, there are many mathematical models that have been used to achieve several purposes for water quality; the common one is the artificial neural network method (ANN), especially with water quality. ANNs have been successfully used with remote sensing technologies for water quality studies [17]. ANN methods have become an effective and popular alternative to conventional methods [18-20]. ANN models have been widely used for water quality problems [21-25]. In this work, the researcher focused on water quality mapping application by remote sensing (satellite) images based on a Hopfield Neural Network (HNN). This application was related with sustainability studies, which are the most important studies in our world.

1.2 Water quality

Water quality is the physical, chemical and biological characteristics of water [26, 27]. The physical characteristics include the colour, temperature and turbidity; the chemical characteristics include the organic and inorganic materials, such as heavy metals, pesticides, petroleum and detergents; and the biological characteristics

include pigment and plankton [28, 29]. It is difficult to define a single water quality standard to meet all uses and user needs. For example, the physical, chemical, and biological parameters of water that are suitable for human usage are different from those of water suitable for irrigating a crop [30]. Deterioration of water quality is a major problem worldwide and often leads to serious environmental impacts and public health concerns [31]. Water quality mapping is an important technique to identify and analyse water pollutants.

1.2.1 Water Quality Mapping

Water quality mapping is the characterization of the location and extent of water features and the relationship of each feature to others. Water quality mapping is considered a valuable tool for spatially distributed assessments of individual quality parameters [32].

Recently, remote sensing has been considered an effective technique for water quality mapping through the analysis of digital images [33]. In water resource research and management, remote sensing applications mainly belong to one of three types [34]:

1. Mapping of watersheds and features.
2. Indirect hydrological parameter estimation.
3. Direct estimation of hydrological variables.

1.2.2 Water Quality Parameters

There are many parameters for the assessment of water quality, and the accredited one or part of them in the investigation depend on the significance of the parameter related with the danger, abundance, and increase in the change of the parameter. In this work, the researcher focused on two parameters, total suspended

solids (TSS) and chlorophyll, because these parameters are very important for the investigated study areas.

1.2.2.(a) **Total Suspended Solids (TSS)**

Total suspended solids (TSS) parameter is commonly considered as a proxy of water quality due to recognised impacts on receiving waters (physical, biological, ecological and eco-toxic). This parameter would be the most significant measurement, as it would depict the effectiveness and compliance of control measures. Therefore, the accurate prediction of TSS loads and concentrations is important in assessing the risk of dangerous conditions in a stream, e.g., due to land-use changes or pollution management strategies [35].

Assessment of the suspended sediment in water bodies is based mainly on the assumption of a uniform distribution of suspended sediments along the water depth [36].

1.2.2.(b) **Chlorophyll**

Chlorophyll is a green pigment found in the cyanobacteria and chloroplasts of algae and plants. The chlorophyll-a concentration is commonly used as a proxy for phytoplankton biomass and as an indicator for eutrophication. Recently, it can be retrieved in water bodies, such as the ocean, rivers, lakes, etc., depending on its physical properties by remote sensing data. Chlorophyll as an indicator of water quality has been detected by remote sensing technologies [37-39]. Several operational monitoring systems based on remote sensing are in place to monitor the open sea and, to some extent, coastal zones. Remote sensing and bio-optical measurements are relatively new techniques that can, in combination with traditional methods, offer more effective management and monitoring of coastal areas [40-42].

1.2.3 Water Quality Assessment

Water quality assessment will become increasingly important as we move into the future; as human populations continue to increase, so too will the amount of pollutants in bodies of water. Testing of water quality is needed worldwide, and the data require frequent updates to remain accurate and relevant. There are a number of different methods to assess water quality data. Usually, this includes linking the elevated pollutant levels with the corresponding cause. Many times, GIS is used to help establish this linkage [43].

1.3 Remote Sensing Techniques

Remote sensing is an art, science, and technology for capturing information from noncontact sensor systems. The freedom from this non-connection enables large amounts of data to be gathered over a small period of time from a single point over a large Area of Interest (AOI) [44]. The term “remote sensing” is most commonly used in connection with electromagnetic techniques of information acquisition. These techniques cover the entire electromagnetic spectrum, including short-wavelength gamma-ray, x-ray, ultraviolet, visible, near infrared, medium infrared, far infrared, and radio waves, through the microwave regions of the spectrum [45]. Figure 1.1 illustrates the electromagnetic spectrum.

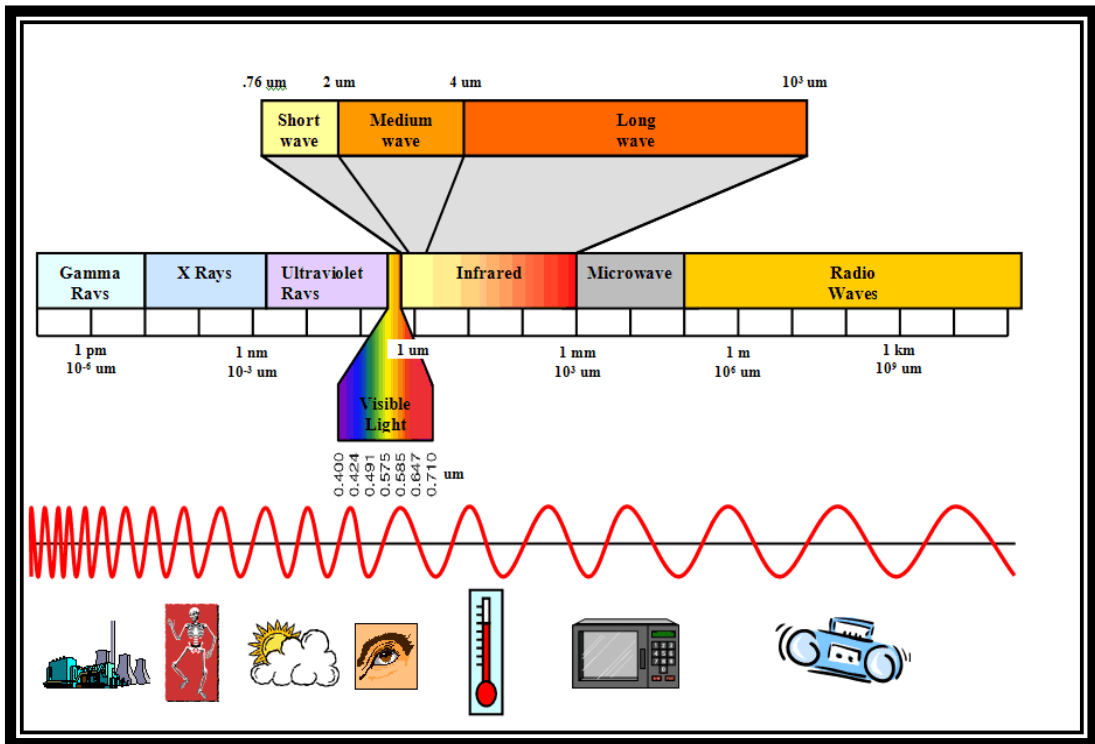


Figure 1.1: Electromagnetic Spectrum.

For this reason, remote sensing has commonly been used to measure the Earth's surface and can include complex, dynamic, distributed systems. The capture of information from the air by satellite or manned aircraft platforms is performed in support of several ecological applications, including water quality [46-49] land cover and land use [50] agriculture [51-57], wildlife management [58, 59], vegetation management [60-62], stream and river management [63-65], and forestry [66-68]. To properly use remotely sensed data, it must be converted into the actionable information needed by end users; otherwise, the data and its acquisition would be worthless [44].

Remote sensing techniques can provide information on both spatial and temporal distributions of key variables [1]. Specifically, these techniques provide very important information on the environmental subsystems of water, air and soil

and their pollution problems. In addition, because water covers approximately three quarters of the Earth and is a major requirement for living creatures, scientists and researchers in the field of remote sensing techniques have great interest in water quality. Therefore, over the last few decades, leaps in remote sensing techniques have enabled unprecedented observations and measurements, achieving fundamental advances in the monitoring of water availability and quality [2]. Point-based assessments of water quality status are not enough to provide information about the spatial coverage of sources of pollution; therefore, remote sensing techniques offer attentively synoptic, repetitive, consistent, cost effective and comprehensive spatio-temporal views [3].

- **Remote Sensing Satellite System**

A satellite is an artificial system that has been intentionally placed in a certain orbit. These objects are sometimes called artificial satellites to distinguish them from natural satellites, such as the Moon. The coming of satellites allows for the acquisition of global and synoptic detailed information about planets (including the Earth) and their environments. Sensors on satellites in the Earth's orbit provide information about global patterns and dynamics of water quality monitoring, clouds, vegetation, land cover/use, seasonal variations, surface morphologic structures, ocean surface temperature, and near-surface wind [45].

The targets in satellite images may be any object or feature that can be observed in the image and have the following characteristics [69]: (a) The targets may be a point, line, or area feature. This means that they can have any form, e.g., a car in a parking lot or a plane on a runway, a house, a bridge or roadway, a large area

of water or a field. (b) The target must be distinguishable; it must have a contrast with other features around it in the image.

1.4 **Artificial Neural Network**

An artificial neural network (ANN) is a computational model based on the structure and functions of biological neural networks. Information that flows through the network affects the structure of the ANN because a neural network changes or learns, in a sense based on that input and output. It processes information using a connectionist approach to computation [70]. Newly developed paradigms of artificial neural networks have strongly contributed to the discovery, understanding and utilization of potential functional similarities between human and artificial information processing systems. Intense research interest persists, and the area continues to develop [71]. ANN conceptions have been used over the last few years and applied to different problem domains, such as finance, medicine, manufacturing, geology and physics [72]. There are many types of artificial neuron networks used in several applications; one of these networks, the Hopfield neural network (HNN), is a special type of artificial neural network that is able to store certain memories or patterns in a manner similar to the brain [73, 74]. It is one of the models that is currently most commonly studied [75, 76] and has the ability to act as an auto-associative memory because of its capability to remember data through observation [77]. HNN is a good technique for solving optimization problems [78, 79]. In this work, a Hopfield neural network has been adapted such that it is convenient for dealing with images that have more than two colours, such as remote sensing (satellite) images.

1.5 Image Classification

Image classification is an important part of remote sensing analysis to identify and classify images. Image classification is a process of transferring the pixels into certain classes. Normally, every pixel is considered as an independent unit that forms the values in the spectrum group. However, the researcher can identify the pixel that enables the comparison of the pixel separately with the known identity in order to make the analysis to group the same pixel into the same classes correspond with the original data [80]. Image classification requires classifiers which are in the form of computer software that can run specific procedures of image classification. Image analysis involves three steps: storage of the image data on a computer for reading, computer manipulation of the data, and output display. Image classification can be separated into two categories supervised classification and unsupervised classification [81].

1.5.1 Supervised Classification

Supervised classification is the procedure most often used for quantitative analysis of remote sensing image data. It rests upon using suitable algorithms to label the pixels in an image as representing particular ground cover types or classes [82]. Therefore, supervised classification methods require extra or external information on the area in the image. Thus, when choosing supervised methods, the user needs to provide some relevant input data before the desired algorithm is applied.

Usually, the information of the input data come from many sources, such as research done on a particular area, data acquired from in-situ, aerial photography, or through the study from the appropriate maps in local or regional level of the interested area. The choice of a good training data set can have a significant

influence on the success of a classification approach. This can be done accurately based on the user's experience in the analysis process [83].

Through the classification, the classes are recognized based on spectral characteristics. The classifiers are software that perform certain operations and are two types that are parametric and non-parametric classifiers. These classifiers differ in the level of their computation complexity. The most effective algorithms require a longer computation time. However, the easiest algorithms can still provide good results in some cases [84].

1.5.2 Unsupervised Classification

In fact, this pattern of classification reverses the supervised classification process. Spectral classes are grouped first based solely on the numerical information in the data, and are then matched by the analyst to information classes (if possible). In other words, unsupervised classification approach is used to cluster pixels in a data set (identifying a group or an original structure in the various spectral data) based on statistics only without any user-defined training classes [85]. This classification process involves algorithms for testing the unknown pixels in the image and gathers them under one class based on the group or original cluster in an image. The purpose of clustering is grouping pixels in intuition unknown numbers of spectral classes. This purpose can be reached through different levels of difficulty and success based on the pixel position in the band space.

Basically, the person running this process should compare the classified data with the reference data (example a map or smaller scale image) to identify the spectral class information in order to map the original classes. Usually the classes are not clear at the early stage even when using supervised classification. The spectral

legends or classes perhaps are too many in one scene that causes a difficulty to train all of them; this is so because the unsupervised classifiers choose the classes automatically.

In this study, the category of the classification by the new algorithm is supervised classification.

Extensive studies based on image classification technique have been carried out for mapping of several phenomena on the earth; some of these studies were recently reviewed by [86]. Therefore, mapping is the most straightforward and mostly related with classification technique.

1.6 Mapping

Generally, maps are the traditional method of storing and displaying geographic information. A map is a graphic representation of the physical features (natural, artificial, or both) of a part or the whole of the Earth's surface, by means of signs and symbols or photographic imagery, at an established scale, on a specified projection, and with the means of orientation indicated. A map portrays three types of information about geographic features [87]:

1. Location and extent of the feature;
2. Characteristics of the feature; and
3. The relationship of the feature to other features.

1.7 The Physical Concept of the Used Image

The current work is related to colour satellite images. This is not only important in giving a view of the physical meaning of this type of image, but also, for the binary image that can be done by Hopfield neural network.

1.7.1 The Physical Concept of the Binary Image

The physical meaning of a binary image is related to its two colours (black and white), while the black colour is represented by (0) as a digital number, and it physically means that the perfect absorption of the object is shown without as not having any reflected light. On the other hand, the white colour is represented by (1) as a digital number, and it physically means there is perfect reflection from the object. This type of image does not give any other value of the reflectance that falls between these two colours. The original object that is represented by this type of image, has a wide range of reflectance for the object represented by these two colours. Therefore, this image is suitable for some purposes such as the result image of the edge detection process, and/or the boundaries map image.

1.7.2 The Physical Concept of the Colour Image

Colour derives from the spectrum of light through the distribution of light power versus wavelength. Colour categories and physical specifications of colour are also associated with objects or materials based on their physical properties such as light absorption, reflection, or emission spectra. By defining a colour space. Colours can be identified numerically by their coordinates [88]. The colour image is considered as a 2-D surface in the 5-D (x, y, Red, Green, Blue) space [89, 90]. It is usually stored in memory as a raster map, a two-dimensional array of small integer triplets; or (rarely) as three separate raster maps, one for each

band. Eight bits per band (24 bits per pixel) seem adequate for most uses, but faint banding artifacts may still be visible in some smoothly varying images, especially those subject to processing.

1.8 Problem Statement

Although the HNN has properties that make it a recognized network among the other artificial neural networks, such as efficiency, simplicity, commonality, and rapidity, it has problems when dealing with multicolour images (images that have more than two colours) because, when an HNN is used with these images, we must convert the wide range of each band, 0-255 (i.e., 256 colours), into a range of two colours (0,1). In this case, information will be lost from the image, especially with satellite images, where each pixel is considered a piece of information that gives understanding about a certain phenomenon. Mutter, in 2010 [91] modified an HNN to create the MHNN algorithm, which deals with colour satellite images by slicing each band into eight binary images called bitplanes and dealing with each bitplane as an independent binary image. This algorithm was applied for water quality by adopting two classes (polluted and unpolluted water) visually. However, this work is not sufficient for water quality mapping (classification) for many reasons. Firstly, MHNN is not a feed-forward auto-associated memory that is suitable for classification purposes; it was adopted as a feed-back (recurrent) auto-associated memory that is used for applications such as enhancement and restoration, so it depended on just two classes that easily gave results but not enough to be accurate for all water classes, where it had problems related with the local minimum, resulting in error and time consumption (as well as the use of a self-connection architecture, which takes more time than a non-self-connection one). In addition, MHNN

considers each bitplane to have the same level, but the levels are not the same, which causes error in the results as well. Secondly, the study did not use validation data to determine the accuracy of the algorithm. Thirdly, MHNN has never been tested with noise or for several satellite images. Fourthly, MHNN cannot estimate pollutant concentrations.

Thus, the researcher decided to develop MHNN to solve the above problems and to introduce an accurate algorithm that addresses the need for satellite image classification in applications of water quality mapping, especially when the water pollutant classification requires increased accuracy compared to other classifications because of the high convergence among the pollutant classes and the dynamic features of water.

1.9 Research Objectives

The main goal of this study is to develop the modified Hopfield neural network (MHNN) algorithm [91] with remote sensing images as classifier for water quality mapping. To achieve this goal, the specific objectives are set as follows:

1. To modify the HNN algorithm to be suitable for satellite images for the classification of water pollutants.
2. To adopt validation data for evaluation of the new algorithm's results.
3. To test the robustness of the new algorithm with noisy images and several types of satellite images.
4. To develop the new algorithm to be capable of estimation of the concentrations values of the pollutants.

1.10 Scope of the Study

This study focused on developing HNN to be appropriate for satellite images, two types of satellite images were used: the first type is Thailand Earth Observation System (THEOS) for Penang strait as the first study area, adopting two different dates, (12-11-2009) and (29-1-2010), where they have (13 samples) and (12 samples) as validation data, respectively, with three bands (red, green, and blue) and with the pixels represented by the digital numbers of these bands in both of these images. The second type is Advanced Land Observation satellite (ALOS) for Langkawi Island coastal waters as the second study area, adopting two different dates (18-1-2010) and a mosaic image formed by two images dates, (18-1-2010) with 12 samples and (26-1-2010) with 13 samples, as validation data, meaning that the mosaic image has (25 samples) of validation data with three bands (blue, green, and red) and that the pixels are represented by the reflectance values of these bands. In addition, the parameters under investigation for water quality mapping are total suspended solid (TSS) in mg/l unit and chlorophyll in mg/m³ unit.

1.11 Thesis Organization

The thesis structure is organized as follows:

Chapter two has two sections. The first section addresses the literature review. It gives supportive background information about this research by presenting previous studies that are related to this research. The second section gives knowledge and information about the Hopfield neural network through mention of its important characteristics, such as its algorithm, applications, and limitations, and also by discussing HNN for colour images and the disadvantages of the last modification of HNN.

Chapter three presents the development of MHNNA for satellite images classification by providing the theoretical explanation for the new algorithm and giving examples of the main network components.

Chapter four explains the methodology of MHNNA classification for water quality mapping by presenting the algorithms used in this work and giving knowledge about the tool adopted in this work.

Chapter five presents the results, discussions, and analyses of the new work.

Chapter six gives the conclusions and recommendations for future work that are related to this study.

CHAPTER TWO

LITERATURE REVIEW AND THE HOPFIELD NEURAL NETWORK

2.1 Literature Review

This section presents previous works that are related to the current work, including works about the Hopfield neural network components, HNN for multicolour images, HNN for colour satellite images, HNN with remote sensing for water quality, and techniques using remote sensing data for water quality mapping.

2.1.1 Hopfield Neural Network Components

Hopfield is name of a physicist who described the Hopfield Neural Network (HNN) during he was working about the magnetic behaviour of solids which is spin glasses [92]. Hopfield neural network is an associative memory, a single layer network, and an interconnected network that have a symmetric learning weight. This net found by J.J. Hopfield in 1982. He explained that the energy, defined by both of the neuron state and the learning weight, the network converges almost the entire pattern from a part of it when the state of the network is at a minimum energy, which denote on the desired pattern. From that time, HNN has attracted many researchers to modify and use it. They used it for applications such as pattern recognition, hardware realization and implementation [93].

Many interesting features of Hopfield neural network have made it use in various applications, where these applications in two ways: analog and digital. HNN can also be used either for optimization problems or as an associative memory via minimization of energy function. Even though, the extensive studies of HNN, there is

still scope for research because it still has limitations. So, it may be used in some applications through conjunction with other neural network models [94].

The last works have adopted and adapted many techniques for HNN. These techniques are related with vector size and HNN capacity, self-connection architecture, feedforward network, local minimum, time of network performance, energy function, HNN for multicolour images, and HNN with remote sensing image for water quality.

2.1.1.(a) **Vector Size and HNN Capacity**

The vector is essential component in the HNN, and its size is related to the memory capacity, which means the ability of storing an amount of information and converging the required information with a minimum cross-talking. mainly the capacity of information depends on the pattern size [95]. For this, several studies have been suggested to improve memory capacity of HNN [96-98] .

There are many studies have introduced improvements to the network capacity. For example, the researchers Kuo and Zhang (1994) [99], showed that the capacity reaches to zero in case of the probe vectors and stored vectors have random distributions. So, it is important to explore this issue and to improve the capacity of the associative memory. Instead of Hopfield associative memory, they studied a multi order polynomial approximation of the Projection Rule and proved that its storage capacity is higher than that of Hopfield associative memory with the same implementation complexity. Until now, the researcher has observed that these two scientists worked on another neural network that is different from Hopfield neural network. On the other hand, some other researchers have improved all or part of HNN architecture. For example, Liwanag (1997) [100] suggested a technique to

improve the capacity of simple Hebbian pattern associations by adding hidden units. The suggested algorithm was structured to choose potential targets for the hidden layer. The latter helped to keep the net from cross talking effects in case the memory was overloaded. But, Lowe (1999) [95] proposed a form of HNN with N neurons that can store $(N \log N)$ biased patterns. The quantity increases when the bias of the patterns increases as well; but, it decreases when the bias becomes large. Besides, Sulehria and Zhang (2008) [101] introduced improvements in the HNN capacity and in the techniques to achieve higher capacity. These improvements were dependent on the best percentage of patterns per number of required neurons.

More improvements on network capacity; Sudo, Sato, and Hasegawa (2009) [93] suggested an associative memory that is good for the memory size and that adaptively increases with learning patterns. This suggestion is neither redundant nor insufficient with regard to memory size, even in an environment that has available the maximum number of associative pairs, which is unknown before learning.

The recent study of many achievements for the HNN is introduced by Mutter 2010 [91] presented a new HNN technique called the Modified Hopfield Neural Network (MHNN). This technique is based on five important approaches that work together in optimizing HNN efficiency. These five approaches are utilizing a smaller vector size (pattern) of three elements with a self-connection architecture, compressing learned data by indexing the weights, applying HNN for multi-resolution images (colour images), using Run Length Encoding to compress weight data, and employing optical HNN based on optical logic gates. The important achievement of the (MHNN) algorithm is making HNN work with colour images without losing image information by converting the image band from decimal to

binary. MHNN was applied to detect water quality. However, this algorithm is not sufficient for this application because of limitations and problems with the local minimum, time performance, non-sequence levels for keeping the energy function in each bitplane, and lack of validation to evaluate the work accuracy.

2.1.1.(b) **Self-Connection Architecture in HNN**

The proposed discrete-valued neural network architecture by Hopfield (1982) needs zero-diagonal elements in the weight matrix (non-self connection) in such a way that all the neurons connect with each other but not with themselves so that the net is converted to a local minimum of the energy function. As for non-zero-diagonal elements of the weight matrix, it was found in the literature that the self-connection could alter the stability of the minimum energy into a point, depending on the new values of the non-zero elements. In case of a model with positive terms along the diagonal, the net only evolves the patterns that have low energy. The net of an outer-product associative content-addressable memory with non-zero-diagonal elements behaves almost identically to one with zero-diagonal terms. In addition, maximum convergence rates and avoidance of steady-state oscillation can result when the non-zero-diagonal weights are used [102-105]. In 2012, Nils Meins et, al [106] proved the advantage of a zero-diagonal weight matrix (non-self-connection architecture) in the Hopfield Neural Network (HNN) and ensemble learning for Robust Face Detection.

In the current study, zero-diagonal weights (non-self-connection) will be adopted to attempt to overcome part of the time consumption problem, and the net will be used for classification without the non-zero-diagonal weight matrix (self-connection architecture).

2.1.1.(c) Hopfield as Feedforward Network

The Hopfield neural network as feedforward has been introduced, but it is rarely, for instance; in 1988, B. Kosko [107] showed that Hopfield feedforward associative memory is a special case of more general feedback Bidirectional associative memories (BAM) and that every real matrix is a BAM. A bidirectional memory is a two-layer neural network and may correspond to a type of S. Grossberg's adaptive resonance. In 2012, Imad [108] modified a Hopfield neural network based on feedforward to detect corresponding patterns, naming the result the Multi-Connect Architecture (MCA), and via his new technique, this researcher solved the local minimum problem, reducing the time performance of HNN and the size of the pattern and dealing with noise. This contributes to a new RTVTM module for suitable demands of a real-time conditional traffic light for recognizing a multitude of vehicles on the road, where the used images (binary images) are produced by edge detection to recognize a number of vehicles in the street in real-time images. This means that, even with all these contributions, this algorithm could not deal with colour images for applications such as segmentation or classification that require all band ranges (not just the two colours produced by edge detection) to recognize each homogenous region in the image to obtain the classes properly.

2.1.1.(d) Energy Function

The energy function is an important concept in HNN, many researchers have modified and improved it to give better results, for example: in 1992, Mitsuo Takeda and Takaaki Kishigami [109] suggested a Hopfield-like energy function with a complex phase-conjugate neural network and gave the physical interpretation for its

dynamics. The suggested model could change the phase amplitudes. They found that the phase-conjugate property was necessary for the optical-gain medium. Their results showed the theoretical prediction of the complex neural fields mechanism. Additionally, in 1994, Lee et al. [110] modified an energy function of a Hopfield neural network to solve the stereo correspondence problem; this modification has been used to provide the 3D structure of a scene. The new network has been applied with real images and random-dot stereograms to prove its efficiency. In 1998, Dong-Chul Park and Seung-Eok Choi [111] proposed a modified energy function for the Hopfield neural network as a recurrent method to obtain the routing order between a source and several destinations, and they used the new version of Hopfield neural network to find the directions in large-scale communication networks. Their approach's results demonstrated the improvements in both computational performance and solution optimality over those of the traditional approach. Additionally, in 2008, Mou et al. [112] formulated a new type of function of Hopfield neural networks in terms of a Linear Matrix Inequality (LMI) to study the problem of global asymptotic stability for delayed Hopfield neural networks (HNNs). They used a fractioning approach to be much less conservative by thinning the delay fractioning, and the advantage and the effectiveness of their approach were demonstrated by a given example.

There are many methods that consider hybrid methods that mix between two or more techniques; in 2010, Subiyanto et al. [113] modified the energy function of a Hopfield neural network-optimized Fuzzy Logic Controller (FLC) to use for maximum power tracking of photovoltaic (PV) energy harvesting systems. The HNN was used to automatically tune the FLC membership functions without the need for trial-and-error. The results in both the simulation and experimental parts proved the

performance and effectiveness of the proposed technique and that it can yield accurate tracking of the maximum power point and improved efficiency of PV systems. In 2012, Anuar M. et al. [114] described a new parameter with energy function of Hopfield neural network for using the sensitivity of this network in super-resolution mapping with a study of the phenomenon of several parameter settings and landscape types, and also, using simulated and real data sets. The success of their work shows that equally weighted parameter settings and imbalanced settings for finding the zone limits are mostly suitable for landscapes comprising large and small patches, respectively.

2.1.2 HNN for Multicolour Images

In previous studies, the interest was focused on conforming HNN to colour images rather than binary images. Essentially, HNN can only deal with two bipolar values (-1, +1). Despite that fact, HNN holds many advantages in image pattern recognition, it just does not function properly with gray or colour levels. Hence, many researchers have paid too much attention to dealing with such a shortcoming by presenting different solutions [115-118]. Badie and Ersoyy (1995) [119] displayed how a multistage HNN approach is used to restore noisy bi-level images that can be considered to solve the problem of error minimization. The multistage technique aimed to push the error function to a deeper minimum than the one reached by the classical single stage of HNN. Although the odd-even splitting is the most ideal natural choice, natural extensions would include splitting the network into (n) sub-networks such that the image reception is adapted to the speed of the machine. The network is divided via a sub-networks method where each level is split into odd-even data. As reported by Zurada et al. (1996) [120], HNN with fully connected standard neurons can be generalized by replacing bi-level activation functions with their

multilevel counterparts with a sigmoidal energy function. The applicability of the network was displayed for a gray-level image restoration where each neuron is considered as one of eight values. The proposed network functions as a multi-stable memory cell and has great potential as an information storage element in which a multiplicity of logic levels can be stored.

Contrary to a single-layer scheme of HNN, Young, Scott, and Nasrabadi (1997) [121] presented an object recognition approach based on concurrent coarse-and-fine matching using a multilayer HNN. The proposed network comprises many cascaded single-layer models of HNN in such a way that an encoded object has a distinct resolution with bidirectional interconnections that link adjacent layers. The interlayer feedback feature of the algorithm reinforces the usual intra-layer matching process in the conventional single-layer models of HNN, with a view to compute the most consistent model across several resolution levels. The algorithm is designed with a focus on performance to test images that contain single objects and multiple occluded objects. The results were compared with recognition results obtained using a single-layer HNN.

Currently, many researchers are showing interest in complex-valued neural networks in different fields and applications, such as optoelectronics, remote sensing, and artificial neural information processing. One of the most crucial features of complex-valued neural networks is the proper treatment of colour image processing [122-125].

Based on previous studies, we believe that there is a need for a new method to split images that have more than two colours into bitplanes. In this manner, HNN with a smaller vector size and non-self-connection architecture can be applied for